

# Benzylic Lithium Compounds: The Missing Link in Carbon–Lithium Covalency. Dynamics of Ion Reorientation, Rotation around the Ring–Benzyl Bond, and Bimolecular C–Li Exchange

Gideon Fraenkel\* and Kevin V. Martin

Contribution from the Department of Chemistry, The Ohio State University,  
120 W. 18th Avenue, Columbus, Ohio 43210

Received June 8, 1995<sup>⊗</sup>

**Abstract:** Benzyl lithium compounds, hitherto assumed from NMR data to consist of ion pairs, have been found to exhibit spin coupling between  $^{13}\text{C}$  and directly bound  $^6\text{Li}$  under conditions wherein bimolecular carbon–lithium bond exchange is too slow to average the coupling constants. These conditions involved the use of species in which lithium is internally solvated or of dilute solutions (0.005 M) of benzyl lithium- $^{13}\text{C}$ - $^6\text{Li}$  (enriched at  $\text{C}_\alpha$ ) at low temperature. The low values of  $^1J(^{13}\text{C}-^6\text{Li})$ , 3–4 Hz, imply a small detectable degree of C–Li covalency with the arrangement around  $\text{C}_\alpha$  distorted from coplanarity. The C–Li bonds in benzyl lithium are concluded to lie in a continuum of C–Li covalency between the many monomeric species in which  $^1J(^{13}\text{C}-^6\text{Li})$  is  $16 \pm 1$  Hz and separated ion pairs. NMR line shape analysis of data for internally solvated benzyl lithium **2b** provides quantitative insight into the dynamics of intramolecular reorientation of coordinated lithium with respect to the benzyl plane, rotation around the ring– $\text{C}_\alpha$  bond, and bimolecular carbon–lithium bond exchange, listed in order of widely different increasing rates, the activation parameters being  $\Delta H^\ddagger$  (kcal/mol) and  $\Delta S^\ddagger$  (eu) in the same order: 14 and 6.6; 6.4 and –14; 10.8 and –21.

At low temperature, 150–180 K, conditions under which bimolecular carbon–lithium bond exchange is slow, many organolithium compounds in solution exhibit spin coupling between  $^{13}\text{C}$  and directly bound lithium.<sup>1–3</sup> Lithium-7 cannot be used because often  $^7\text{Li}$  electric quadrupole induced relaxation is sufficiently fast to average the  $^{13}\text{C}$ – $^7\text{Li}$  coupling constant.<sup>1</sup> However,  $^6\text{Li}$  relaxation is slow enough<sup>4</sup> to allow observation of  $^1J(^{13}\text{C}-^6\text{Li})$ . Among a wide variety of organolithium compounds,  $\text{R}_n\text{Li}_n$ , solvated and unsolvated,  $\text{R} = \text{alkyl, vinyl, aryl, alkynyl, heterocycle}$ ,  $n = 1, 2, 4, \text{ and } 6$ , the one-bond  $^{13}\text{C}$ – $^6\text{Li}$  coupling constants fall into a remarkable common pattern (1).<sup>5</sup> They depend largely on the state of aggregation,  $n$ , and

$$^1J(^{13}\text{C}-^6\text{Li}) \approx 16.5/n \quad (1)$$

hardly at all on the nature of the organic moiety. While this result may be rationalized, see below, a satisfactory explanation for it has not yet been fully established. Then, there are the compounds for which carbon–lithium coupling has not been observed. Its absence may be due to insufficient “s” character<sup>7–11</sup> associated with some carbon–lithium covalency, or just insuf-

ficient covalency. The latter condition applies to solvent-separated ion pairs of lithium carbanide salts.<sup>12</sup>

Finally, it is always possible that the absence of observable  $^{13}\text{C}$ – $^6\text{Li}$  coupling is due to fast intermolecular C–Li bond exchange.<sup>1–3</sup> Such an effect can be confirmed if  $^{13}\text{C}$ – $^6\text{Li}$  coupling is observed at reduced temperatures. If coupling or selective  $^{13}\text{C}_\alpha$  line broadening (removed by  $^6\text{Li}$  irradiation) fails to materialize at the lowest temperatures commensurate with obtaining acceptable spectra, then fast exchange cannot be eliminated.

One might imagine that a continuum of increasingly ionic C–Li bonds would be experimentally manifested by a series of decreasing one-bond  $^{13}\text{C}$ – $^6\text{Li}$  coupling constants. Such an observation has not been reported. There are very few one-bond  $^{13}\text{C}$ – $^6\text{Li}$  coupling constants which fall outside the common pattern (1).<sup>14,15</sup> However, a new and unexpected example of “missing link”  $^{13}\text{C}$ – $^6\text{Li}$  coupling behavior has been found, and that is the subject of this paper. Below are described several

(8) (a) McConnell, H. M. *J. Chem. Phys.* **1956**, *24*, 460. (b) Muller, N.; Pritchard, D. E. *J. Chem. Phys.* **1959**, *31*, 768. (c) Muller, N.; Pritchard, D. E. *J. Chem. Phys.* **1959**, *31*, 1471. (d) Muller, N. *J. Chem. Phys.* **1962**, *36*, 359. (e) Pople, J. A.; Santry, D. P. *Mol. Phys.* **1964**, *8*, 1. (f) Galasso, V. *J. Chem. Phys.* **1985**, *82*, 899.

(9) (a) Juan, C.; Gutowsky, H. S. *J. Chem. Phys.* **1962**, *37*, 2198. (b) Pyykko, P.; Wiesenfeld, L. *Mol. Phys.* **1981**, *43*, 557. (c) Kupce, E.; Lukevics, E. *J. Magn. Reson.* **1988**, *76*, 63.

(10) Karplus, M.; Grant, D. M. *Proc. Natl. Acad. U.S.A.* **1959**, *45*, 1269. (11) (a) Grant, D. M.; Litchman, W. M. *J. Am. Chem. Soc.* **1965**, *87*, 3994. (b) Litchman, W. M.; Grant, D. M. *J. Am. Chem. Soc.* **1967**, *89*, 2228.

(12) (a) Swarc, M. *Ions and Ion-Pairs in Organic Reactions*; Wiley-Interscience: New York, 1972; Vol. 1. (b) Hogen-Esch, T. E. *Adv. Phys. Org. Chem.* **1977**, *15*, 153.

(13) (a) Thomas, R. D.; Clarke, M. T.; Jensen, R. M.; Young, T. C. *Organometallics* **1986**, *5*, 1851. (b) Heinzer, J.; Oth, J. F. M.; Seebach, D. *Helv. Chim. Acta* **1985**, *68*, 1848.

(14) Reich, H. J.; Borst, J. P.; Dykstra, R. R. *Tetrahedron* **1994**, *50*, 5869.

(15) Reich, H. J.; Dykstra, R. R. *J. Am. Chem. Soc.* **1993**, *115*, 7041.

<sup>⊗</sup> Abstract published in *Advance ACS Abstracts*, October 1, 1995.

(1) (a) Fraenkel, G.; Fraenkel, A. M.; Geckle, M. J.; Schloss, F. *J. Am. Chem. Soc.* **1979**, *101*, 4745–4747. (b) Fraenkel, G.; Henrichs, M.; Hewitt, J. M.; Su, B. M.; Geckle, J. M. *J. Am. Chem. Soc.* **1980**, *102*, 3345–3350.

(2) (a) Seebach, D.; Hässig, R.; Gabriel, J. *Helv. Chim. Acta* **1983**, *66*, 308. (b) Seebach, D.; Siegel, H.; Gabriel, J.; Hässig, R. *Helv. Chim. Acta* **1980**, *63*, 2046–2053.

(3) (a) Fraenkel, G.; Hsu, H.-P.; Su, B. M. In *Lithium Current Applications in Science Medicine and Technology*; Bach, R. O., Ed.; Wiley: New York, 1985; p 273. (b) Fraenkel, G. In *Recent Advances in Anionic Polymerization*, Hogen-Esch, T., Smid, J., Eds.; Elsevier: New York, 1987; p 23.

(4) Wehrli, F. W. *J. Magn. Reson.* **1978**, *30*, 193.

(5) Bauer, W.; Winchester, W. R.; Schleyer, P. v. R. *Organometallics* **1987**, *6*, 2371–2379.

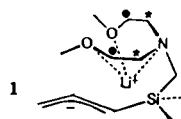
(6) Bauer, W.; Griesinger, C. *J. Am. Chem. Soc.* **1993**, *115*, 10871.

(7) Ramsey, N. F. *Phys. Rev.* **1953**, *91*, 303.

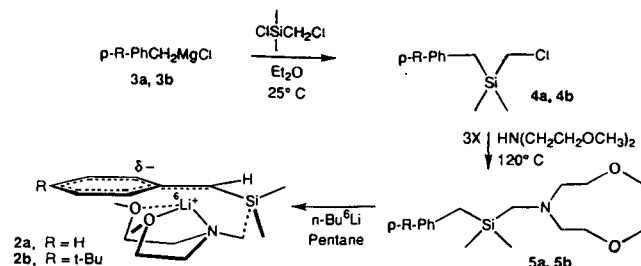
benzylic lithium compounds which exhibit intermediate  $^{13}\text{C}$ – $^6\text{Li}$  spin coupling as well as a variety of dynamic behaviors, indicating intramolecular reorientation of coordinated lithium with respect to the carbanionic moiety, rotation about the ring–benzyl bond, and intermolecular C–Li bond exchange.

## Results and Discussion

In previous work we have described several examples of allylic organolithium compounds, currently believed to be contact ion pairs, within which, according to our NMR data, reorientation of ions with respect to each other is slow relative to the NMR time scale at 160 K.<sup>16</sup> For example, **1** was shown



to assume the folded structure, since at 160 K all carbons on the pendant ligand are magnetically nonequivalent.<sup>16c</sup> Then above 160 K signal averaging of the  $^{13}\text{C}$  NMR doublets, due to the pairs of ligand carbons labeled with stars and dots, to single lines at their respective centers was proposed to be the result of transfer of coordinated lithium between two sides of the allyl plane.<sup>16c</sup> The  $\Delta H^\ddagger$  values for this intramolecular ion–ion reorientation process in this and several related systems are all around 7 kcal/mol with  $\Delta S^\ddagger$  of  $\pm 8$  eu.<sup>16</sup> Such sluggish motion was not expected from theory. We now present the analogous experiments using substituted benzyllithiums, for example, **2a**. If this species adopts the folded structure, shown, then all carbons, especially methylsilyl carbons and those in the ligands, should be magnetically nonequivalent. Studies analogous to those for **1**<sup>16c</sup> should provide the dynamics of intramolecular ion–ion reorientation. As shown below, effects such as these have now been seen for **2a** and a substituted model, **2b**.



Compound **2a** was prepared as shown via transformation of **3a** to **5a** followed by metalation of **5a** using *n*-butyllithium- $^6\text{Li}$  in diethyl ether/pentane at room temperature. This yielded a precipitate of **2a**, >95% pure by NMR analysis; see the Experimental Section. Carbon-13 NMR of this compound in THF- $d_8$  exhibited nonequivalent *ortho* carbons, implying slow rotation around the ring–benzyl bond, discussed below; see Chart 1. The resonances for methoxy,  $\text{NCH}_2\text{C}$ , and  $\text{CH}_3\text{Si}$  carbons broaden, considerably with decreasing temperature to 200 K, compared to other lines in the spectrum. Below 200 K the sample precipitated from solution. This behavior is consistent with a slowing at reduced temperatures of the rotation of coordinated lithium around the benzyl–silicon bond in proposed structure **2a**. At sufficiently slow rotation all carbons in the pendant ligand should become magnetically nonequivalent;

(16) (a) Fraenkel, G.; Winchester, W. R. *J. Am. Chem. Soc.* **1990**, *112*, 1382–1386. (b) Fraenkel, G.; Chow, A.; Winchester, W. R. *J. Am. Chem. Soc.* **1990**, *112*, 2582–2585. (c) Fraenkel, G.; Cabral, J. *J. Am. Chem. Soc.* **1993**, *115*, 1551–1557. (d) Cabral, J.; Fraenkel, G. *J. Am. Chem. Soc.* **1992**, *114*, 9067–9075.

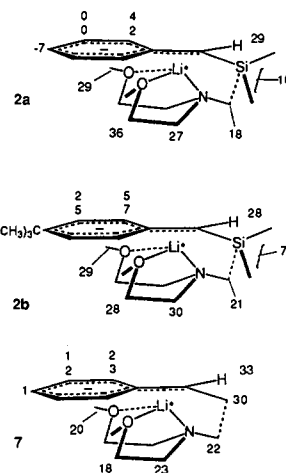
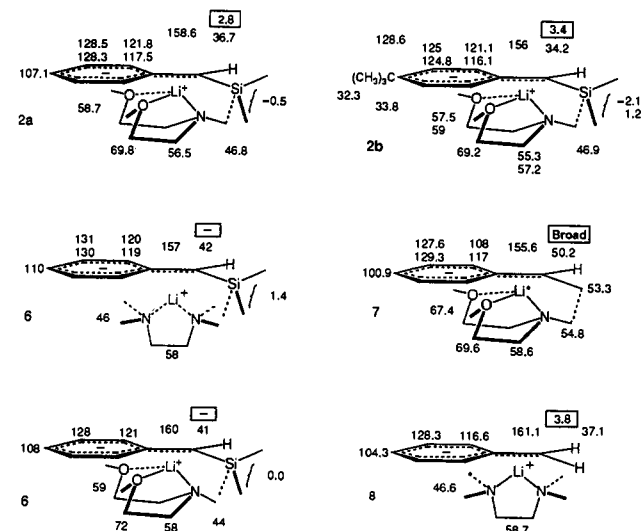


Figure 1. NOE enhancements,  $^6\text{Li}\{^1\text{H}\}$ , in compounds **2a**– $^6\text{Li}$ , **2b**– $^6\text{Li}$ , and **7**– $^6\text{Li}$ , 0.8 M, in THF- $d_8$  at 220 K.

Chart 1.  $^{13}\text{C}$  NMR Benzyllithium Compound Shifts,  $\delta$  ( $^1J(^{13}\text{C}_\alpha$ – $^6\text{Li})$  Hz in Boxes)



evidently the sample does not remain in solution down to the required low temperature.

On the assumption that a ring-substituted version of **2a** would be more soluble than **2a** at low temperature, the 4-*tert*-butyl analog **2b** was prepared; see **3b**–**2b**. At 180 K  $^{13}\text{C}$  NMR of this compound in THF- $d_8$  exhibited nonequivalent *ortho*, methoxy,  $\text{NCH}_2\text{C}$ , and  $\text{CH}_3\text{Si}$  carbons, each pair appearing as a clean 1:1 doublet; see Chart 1. Above 180 K with increasing temperature, these doublets progressively average to single lines at their respective centers; see below. These observations are consistent with the proposed folded structure and the suggestion that  $^{13}\text{C}$  NMR line shape changes are the result of dynamics of transfer of lithium with ligand between two sides of the benzyl plane. Interestingly at 200 K the ligand  $^{13}\text{C}$  resonances of **2a** and **2b** have very similar shapes.

In addition to the above described behavior the results of NOE experiments,  $^6\text{Li}\{^1\text{H}\}$ , on **2a** and **2b** in THF- $d_8$  clearly establish the proximity of lithium to ligand protons, Figure 1.

The most unexpected observation in the  $^{13}\text{C}$  NMR of **2a** and **2b** is spin coupling between benzyl  $^{13}\text{C}_\alpha$  and directly bonded lithium, both with  $^6\text{Li}$  and  $^7\text{Li}$ . At 250 K the  $^{13}\text{C}$  NMR of **2a**– $^7\text{Li}$  in THF- $d_8$  is an equal quartet with  $^1J(^{13}\text{C}$ – $^7\text{Li})$  of 7.4 Hz while for the  $^6\text{Li}$  isotopomer the resonance is an equal triplet,  $^1J(^{13}\text{C}$ – $^6\text{Li})$  of 2.8 Hz. The ratio of the coupling constants 2.64 matches that of the corresponding lithium resonance frequencies,

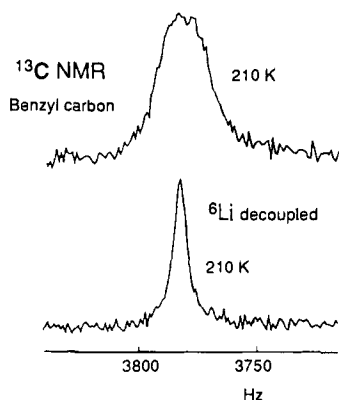
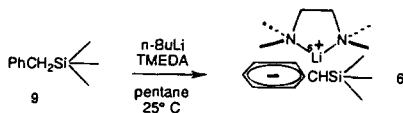


**Figure 2.**  $^{13}\text{C}_\alpha$  NMR of **7**, 0.4 M, in THF- $d_8$  with and without  $^6\text{Li}$  decoupling.

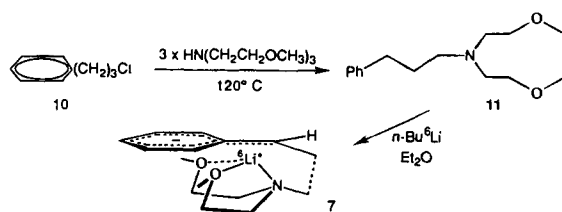
2.641, as expected. Ordinarily  $^7\text{Li}$  quadrupole induced relaxation in most organolithium compounds is fast enough to average the  $^{13}\text{C}$ - $^7\text{Li}$  coupling.<sup>13,17</sup> Apparently in **2a** the electric field gradients are uncharacteristically small. Needless to say,  $^{13}\text{C}_\alpha$ - $^6\text{Li}$  coupling is also seen using THF- $d_8$  solutions of **2b** at 250 K; see Chart 1.

The ligand  $^{13}\text{C}$  resonances of **2a** and **2b**, their temperature dependent line shapes, and their NOE behavior together with the observation of  $^{13}\text{C}_\alpha$ -lithium spin coupling complete establishment of their proposed folded structures.

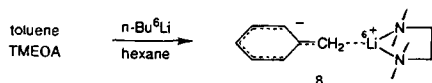
To further investigate this unusual  $^{13}\text{C}_\alpha$ - $^6\text{Li}$  spin coupling, three more benzylic lithium compounds were prepared—[ $\alpha$ -(trimethylsilyl)benzyl]lithium **6**, a carbon analog of **2a**, **7**, and



benzyl lithium<sup>8</sup> itself. Metalation of precursor **9**, **11**, and toluene with  $n\text{-Bu}^6\text{Li}$  in the presence of different ligands furnished,



respectively, solutions of **6**- $^6\text{Li}$ , **7**- $^6\text{Li}$ , and benzyl lithium **8**- $^6\text{Li}$ .



Precursor **11** was prepared from **10**. Neither sample of **6**, prepared in the presence of TMEDA or bis(2-methoxyethyl)-*N*-methylamine, showed evidence of  $^{13}\text{C}$ - $^6\text{Li}$  coupling down to 200 K. The latter preparation is the ligand-detached version of **2a**. Selective broadening of the *N*-methylene resonance seen at 200 K in the  $^{13}\text{C}$  NMR of **6** with TMEDA implies some TMEDA is complexed to lithium.

In the case of the carbon analog **7**- $^6\text{Li}$ ,  $^{13}\text{C}_\alpha$  NMR at 220 K consisted of a broad line. The latter narrowed on decoupling

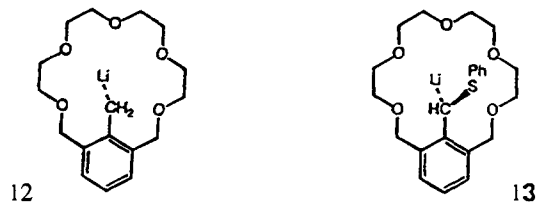
(17) (a) Reviewed by Bauer, W.; Schleyer, P. v. R. In *Advances in Carbanion Chemistry*; Sniekus, V., Ed.; Jai Press: Greenwich, CT, 1992; Vol. 1, pp 81–175. (b) Gunther, H.; Moskau, D.; Bast, P.; Schmalz, D. *Angew. Chem., Int. Ed. Engl.* **1987**, *26*, 1212. (c) Thomas, R. D. In *Isotopes in the Physical and Biomedical Sciences*; Jones, J. R., Buncel, E., Eds.; Elsevier: Amsterdam, 1992; p 367.

$^6\text{Li}$ , see Figure 2, implying  $^{13}\text{C}_\alpha$  is coupled to  $^6\text{Li}$  here also. In addition, the results of an NOE experiment,  $^6\text{Li}\{^1\text{H}\}$ , clearly establish the proximity of  $^6\text{Li}$  to ligand protons, Figure 1.

Benzyl lithium- $^6\text{Li}$  at 180 K in THF- $d_8$  with TMEDA gave a sharp single  $^{13}\text{C}_\alpha$  resonance, indicating no observable  $^{13}\text{C}_\alpha$ - $^6\text{Li}$  spin coupling. This sample did not show some broadening of the TMEDA methylene  $^{13}\text{C}$  resonance, by 200 K.

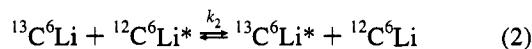
All the samples discussed so far showed very similar ring  $^{13}\text{C}$  NMR shifts, see Chart 1. Their alternating character, shielding at the *ortho* and *para* carbons relative to  $\delta$  *ca.* 128 at the *meta* carbons, is most reasonably ascribed to some negative charge delocalized into the aromatic rings.<sup>18</sup> Similar  $^{13}\text{C}$  shifts implies similar electronic structures and that all species in Chart 1 are subjected to  $^{13}\text{C}$ - $^6\text{Li}$  coupling, and most likely this applies to all secondary benzyl lithiums as well as benzyl lithium itself. Then, whether or not  $^{13}\text{C}_\alpha$ - $^6\text{Li}$  coupling is observed depends on the rate of bimolecular  $\text{C}_\alpha$ -Li bond exchange. In the case of **2a** and **2b**, the process is slow enough to reveal  $^{13}\text{C}_\alpha$ - $^6\text{Li}$  spin coupling due to the encapsulated sites of lithium. This would render the exchange process to be energetically unfavorable due to steric interactions in the transition state.

In support of the above findings and conclusions, two internally solvated benzylic lithiums, **12** and **13**, were recently

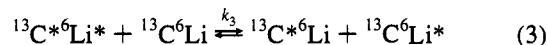


reported to exhibit  $^1J(^{13}\text{C}$ - $^7\text{Li})$  values of 7.0 Hz for **12** and 9 Hz for **13**.<sup>19</sup> Evidently encapsulation of lithium here also renders carbon lithium exchange slow enough to reveal the  $^{13}\text{C}_\alpha$ - $^7\text{Li}$  coupling.

We now turn to the case of benzyl lithium. If the absence of observable  $^{13}\text{C}_\alpha$ - $^6\text{Li}$  coupling is due to fast intermolecular C-Li exchange, decreasing the rate should reveal the coupling. That could be accomplished by lowering the temperature and/or reducing the concentration, subject to the following practiced limitations. Below 180 K the material precipitates from THF- $d_8$  solution. Using solutions of benzyl lithium, with  $^{13}\text{C}$  in natural abundance, at concentrations less than 0.1 M results in unsatisfactory  $^{13}\text{C}$  NMR data. A 0.1 M solution is *ca.*  $1.1 \times 10^{-3}$  M in benzyl moieties containing  $^{13}\text{C}_\alpha$ . The carbon-lithium bond exchange step responsible for averaging the  $^{13}\text{C}_\alpha$ - $^6\text{Li}$  coupling may be abbreviated as



*i.e.*, there is mutual exchange of  $^6\text{Li}$ 's between a  $^{12}\text{C}_\alpha$  and a  $^{13}\text{C}_\alpha$ . The slower step is exchange of lithiums between two  $^{13}\text{C}_\alpha$ 's (3). The exchange rate for the above sample would be



*ca.*  $1.1 \times 10^{-4}k_2$ , due mainly to (2). A sample of benzyl lithium- $^{13}\text{C}$ - $^6\text{Li}$ ,  $1.1 \times 10^{-3}$  M, would have the same  $^{13}\text{C}_\alpha$  NMR signal/noise ratio as that from the above 0.1 M sample with  $^{13}\text{C}$  in natural abundance, but its  $\text{C}_\alpha$ -Li exchange rate due to (3) would be slower by a factor of *ca.* 100. Accordingly samples were

(18) (a) Spiess, H.; Schneider, W. G. *Tetrahedron Lett.* **1961**, 468. (b) O'Brien, D. H.; Hart, A. J.; Russell, C. R. *J. Am. Chem. Soc.* **1975**, *97*, 4410. (c) Tokuhito, T.; Fraenkel, G. *J. Am. Chem. Soc.* **1969**, *91*, 5005. (19) Ruhland, T.; Hoffmann, R. W.; Schade, S.; Boche, G. *Chem. Ber.* **1995**, *128*, 551–556.

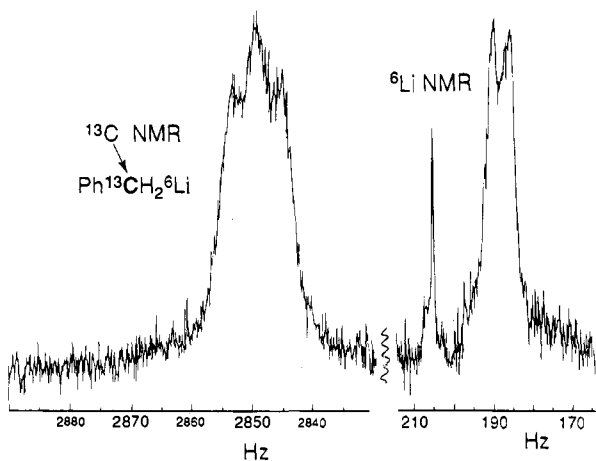


**Figure 3.** (left) NMR of benzyl lithium- $^{13}\text{C}_\alpha\text{-}^6\text{Li}$ , 0.005 M, with 0.005 M TMEDA in THF- $d_8$ . (right) Same sample  $^6\text{Li}$  NMR at 180 K.

prepared by benzyl lithium- $^{13}\text{C}_\alpha\text{-}^6\text{Li}$  by deprotonation of toluene- $^{13}\text{C}_\alpha$  with *n*-butyllithium- $^6\text{Li}$  in a mixture of pentane and TMEDA at room temperature. A solution of this compound,  $8\text{-}^{13}\text{C}_\alpha\text{-}^6\text{Li}$ ,  $5 \times 10^{-3}$  M, in THF- $d_8$  solution at 180 K displayed an equal triplet for  $^{13}\text{C}_\alpha$  NMR and a 1:1 doublet in  $^6\text{Li}$  NMR, the splitting in both spectra being 3.8 Hz; clearly this is due to  $^{13}\text{C}_\alpha\text{-}^6\text{Li}$  coupling (see Figure 3). This kinetic device to reveal a coupling constant by use of dilute samples of strategically isotopically enriched compounds, at low temperature, has been used before,<sup>1,20</sup> though without adequate explanation.

Regarding the role of TMEDA in this preparation, HOESY experiments have already established  $^6\text{Li}$  to be complexed to TMEDA. No NOE contacts were observed between  $^6\text{Li}$  and ring hydrogens.<sup>19</sup>

It is now appropriate to consider the origin and magnitude of the  $^{13}\text{C}_\alpha\text{-}^6\text{Li}$  coupling in benzyl lithiums: In their treatment of the Fermi contact contribution to spin coupling between directly bonded atoms,<sup>7</sup> using electron pair theory, Karplus, Grant, and Lichtman<sup>10,11</sup> derived the relationship

$$^1J(^{13}\text{C}\text{-}^1\text{H}) \propto \gamma_C \gamma_{\text{H}} s^2 Z^3 \quad (4)$$

where  $s^2$  is the "s" character associated with the CH bond orbital and  $Z$  is the effective nuclear charge, a function of the C-H covalence. Thus, the observed dependence of most  $^1J(^{13}\text{C}\text{-}^1\text{H})$  values on the "s" character reasonably implies that the C-H covalent character is constant.<sup>21</sup> For the wide variety of organolithium compounds, among which the  $^1J(^{13}\text{C}\text{-}^6\text{Li})$  values depend only on the state of aggregation, one has to conclude that the factor  $s^2 Z^3$  is constant; i.e., the "s" character is inversely proportional to the C-Li covalence.<sup>6,21</sup> Among the many "common pattern" monomers,  $^1J(^{13}\text{C}\text{-}^6\text{Li})$  is  $16 \pm 0.5$  Hz.<sup>5</sup> The corresponding coupling constants for benzyl lithium and its analogues studied here are all around 2.5–4 Hz. In these species, our data, together with results from X-ray crystallography, place lithium above  $\text{C}_\alpha$  and normal to the partly delocalized  $\pi$  plane.<sup>22</sup> Such a bonding arrangement would have less associated "s" character than that in the "common pattern" monomers. On the basis of previous and current results, it is

(20) Seebach, D.; Gabriel, J.; Hässig, R. *Helv. Chim. Acta* **1984**, *67*, 1083.

(21) (a) Lambert, C.; Schleyer, P. v. R. *Angew. Chem., Int. Ed. Engl.* **1994**, *33*, 1129. (b) Van Eikema Hommes, N. J. R.; Schleyer, P. v. R. Unpublished results.

(22) (a) Zarges, W.; Marsch, M.; Harms, K.; Boche, G. *Chem. Ber.* **1989**, *122*, 2304. (b) Zarges, W.; Marsch, M.; Harms, K.; Koch, W.; Frenking, G.; Boche, G. *Chem. Ber.* **1991**, *124*, 543. (c) Patterman, S. P.; Karle, I. L.; Stucky, G. D. *J. Am. Chem. Soc.* **1970**, *92*, 1150. (d) Beno, M. A.; Hope, H.; Olmstead, M. M.; Power, P. P. *Organometallics* **1985**, *4*, 2117.

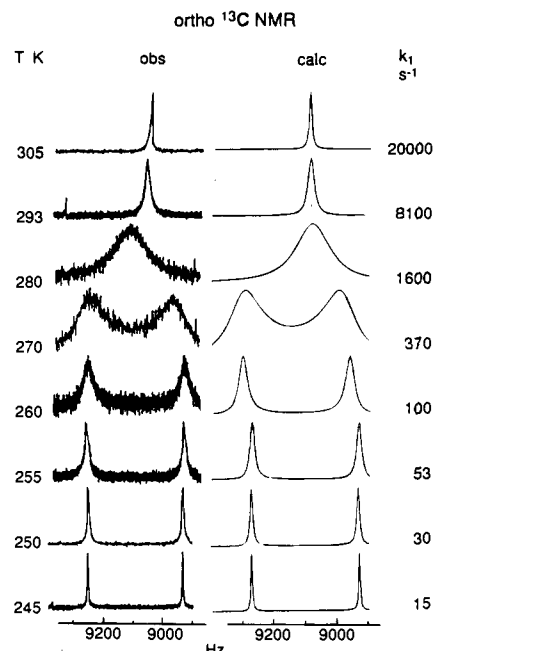


**Figure 4.** (left)  $^{13}\text{C}$  NMR of **2a**, 0.075 M, in THF- $d_8$ , *ortho* carbons at different temperatures. (right) Calculated line shapes with first-order rate constants.

tempting to propose that the ionic characters of the  $\text{C}_\alpha\text{-Li}$  bonds in these benzyl lithiums lie somewhere between that for the common pattern species and the truly separated ion pairs, the missing link along what should be a monotonically decreasing range of C-Li bond covalencies.

These conclusions are supported by the results of X-ray crystallographic studies of benzyl lithium complexed to different donors<sup>22a,c,d</sup> as well of  $6\cdot\text{TMEDA}$ .<sup>22b</sup> Lithium is above  $\text{C}_\alpha$  and normal to the benzyl plane. In  $8\cdot\text{TMEDA}\cdot\text{THF}$ <sup>22a</sup> and  $6\cdot\text{TMEDA}$ <sup>22b</sup> a pyramidal structure was noted around  $\text{C}_\alpha$  with substituents *ca.*  $13^\circ$  below the benzyl plane (opposite lithium) in the former compound, and in the latter, the angles for  $\text{C}_\alpha\text{-H}$  bonds are  $15^\circ$  and  $17^\circ$ .<sup>22a</sup>

As indicated above, several of the benzyl lithiums described here exhibited in their  $^{13}\text{C}$  NMR spectra interesting line shape changes, indicating the operation of different dynamic effects. Several **2a**, **2b**, and **7**, showed nonequivalent *ortho* carbons at low temperature, 240 K. With increasing temperature, these two resonances coalesce and signal average, the result of progressively faster rotation around the ring-benzyl bond. Such is the case for **2a**; see Figure 4. Similar effects are seen in the resonances for the *meta* carbons. Comparison of experimental<sup>23</sup> spectra with line shapes calculated to fit the data provides the rates of reaction used in the Eyring plot, Figure 5; the resulting activation parameters are listed in Table 1, together with values for compounds **2b** and **7**. These barriers to rotations in benzylic lithium compounds are known to depend on the nature of the lithium ligands present.<sup>24</sup> It has been proposed that the transition states for rotation involve some increase in benzyl carbon-lithium covalence with corresponding diminution of bonding between lithium and ligand.<sup>22</sup>

In the case of [1-(trimethylsilyl)allyl]lithium,  $\Delta H^\ddagger$  values for rotation around the  $\text{CH}_2\text{-CH}$  bond vary with ligand from 10

(23) (a) Gutowsky, H. S.; Saika, A. *J. Chem. Phys.* **1953**, *21*, 1688. (b) Kaplan, J. E.; Fraenkel, G. *J. Am. Chem. Soc.* **1972**, *94*, 2907. (c) Kaplan, J. I.; Fraenkel, G. *NMR of Chemically Exchanging Systems*; Academic Press: New York, 1980; Chapters 5 and 6.

(24) (a) Fraenkel, G.; Geckle, J. M. *J. Am. Chem. Soc.* **1980**, *102*, 2869 and references therein. (b) Albrecht, H.; Harback, J.; Hauck; Kalinowski, H. O. *Chem. Ber.* **1992**, *125*, 1753–1762.

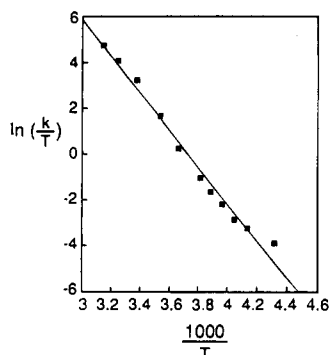


**Figure 5.** Eyring plot for rotation around the ring- $C_{\alpha}$  bond of **2a**, as in Figure 4.

**Table 1.** Activation Parameters

	$\Delta H^{\ddagger}$ (kcal/mol)	$\Delta S^{\ddagger}$ (eu)	$\Delta G^{\ddagger}$ (250 K) (kcal/mol)
Ring-Benzyl Rotation			
<b>2a</b> , <i>meta</i> carbons	16	11.2	13.2
<i>ortho</i> carbons	16.2	12	13.2
<b>2b</b> , <i>ortho</i> carbons	14	6.6	12.3
<b>7</b> , <i>ortho</i> carbons	20.5	19.6	13.6
Ion-Ion Reorientation			
<b>2b</b> , methylsilyl carbons	6.4	-14	9.9
methoxy carbons	7.2	-10	9.7
$NCH_2C$ carbons	6.1	-15	9.9
C-Li Exchange			
<b>2b</b> , $C_{\alpha}$	10.8	-21	16.1

to 14 kcal/mol with entropies around  $\pm 10$  eu.<sup>16b</sup> Interestingly in the case of **1** while the barrier to rotation around  $C_1-C_2$  takes values of *ca.* 15 kcal/mol, dependent on the medium, the process around the  $C_2-C_3$  bonds is too slow to measure using NMR methods up to 340 K.<sup>16c</sup> Thus, the proximity of Li to  $C_1$  in the ground state of **1** favors development of a transition state with some C-Li covalency but not to  $C_3$ . The results of *ab initio* calculations on allyllithium support these proposals.<sup>25</sup>

At the beginning of this paper a proposal was made to use  $^{13}C$  NMR line shape analysis of the ligand carbons of **2a** to elucidate the dynamics of reorientation of coordinated lithium with respect to the benzyl moiety, analogous to the studies of **1**.<sup>16c</sup> These effects were indicated qualitatively for **2a** since only some selective line broadening of ligand  $^{13}C$  resonances was observed. However, at 180 K the  $NCH_2C$ ,  $CH_3O$ , and  $CH_3-Si$   $^{13}C$  resonances of **2b** all consist of 1:1 doublets, consistent with the proposed folded structure. With increasing temperature, each doublet averages to a single line at its center; see Figures 6 and 7. Line shape analysis of all these data,<sup>23</sup> Figure 6 and 7, results in similar rates from all three line shapes at each temperature, implying that the values, the apparent first-order rate constants, are independent of the concentration of **2b**. The resulting activation parameters,  $\Delta H^{\ddagger}$  of 6–7 kcal/mol and  $\Delta S^{\ddagger}$  of -10 to -14 eu, are very similar; see Table 1. Since the methylsilyl resonance is better defined, the resulting activation parameters are more accurate. Altogether these line shape changes are most reasonably the result of transfer of coordinated lithium between two sides of the benzyl plane via rotation around the benzyl carbon-silicon bond. This is analogous to our results for **1**<sup>16c</sup> for which the cation-anion reorientation  $\Delta H^{\ddagger}$  was 7–8 kcal/mol with  $\Delta S^{\ddagger}$  of -15 eu. Similar effects were observed for [1,3-bis(trimethylsilyl)allyl]lithium·TMEDA, (1,1,3,3-tetramethylallyl)lithium·TMEDA, and [1-(trimethylsilyl)allyl]lithium complexed to  $N,N',N'',N''',N''''$ -pentamethyl-di-

(25) Van Eikema Hommes, N. J. R.; Bühl, M.; Schleyer, P. v. R. *J. Organomet. Chem.* **1991**, 409, 307.

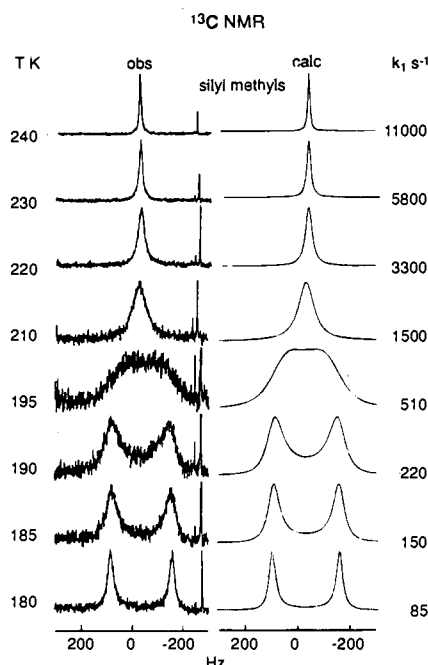


**Figure 6.** (left)  $^{13}C$  NMR of **2b**, 0.086 M, in  $THF-d_8$ , silyl methyls at different temperatures. (right) Calculated line shapes with first-order rate constants.

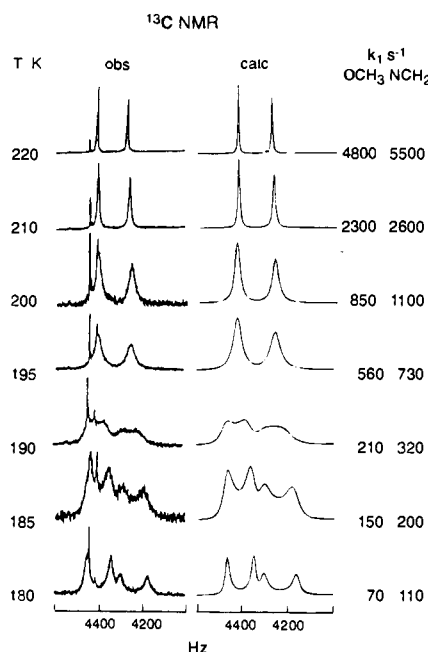


**Figure 7.** (left)  $^{13}C$  NMR of **2b**, as in Figure 6, ligand resonances, methoxy to left of  $NCH_2C$ . (right) Calculated.

ethylenetriamine.<sup>16</sup> The bonding arrangement in the benzyl-lithiums differs from that in the allyllithiums, in that the latter species failed to exhibit  $^{13}C-^6Li$  spin coupling even under conditions when intermolecular exchange of lithiums is slow relative to the NMR time scale. Both systems exhibit line shape changes due to dynamics of reorientation of coordinated Li with respect to the organic moiety. Effects similar to these were reported by Albrecht and Hoffman in their study of ( $\alpha$ -heterobenzyl)lithiums.<sup>26</sup>

The last dynamic effect to be discussed here involves progressive averaging of the  $^{13}C_{\alpha}-^6Li$  coupling constant of **2b-<sup>6</sup>Li** in  $THF-d_8$  with increasing temperature above 270 K. Since

(26) Albrecht, H.; Harbach, J.; Hoffman, R. W.; Ruhland, T. *Liebigs Ann. Chem.* **1995**, 211–216.

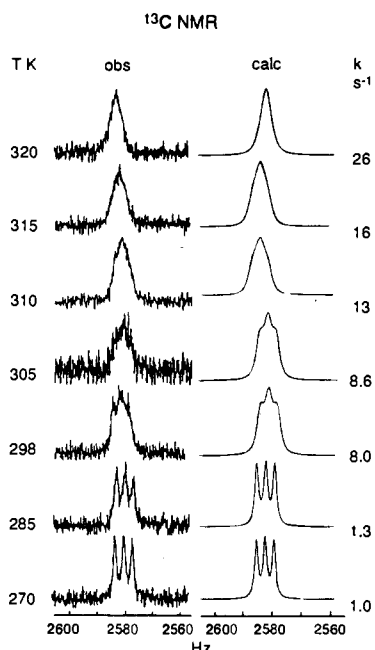
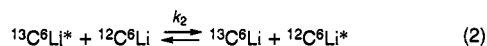


**Figure 8.** (left)  $^{13}\text{C}_\alpha$  NMR of  $2\text{b-}^6\text{Li}$ , in  $\text{THF-}d_8$  at different temperatures. (right) Line shapes calculated to fit the data, modeled as bimolecular C–Li exchange.

$^6\text{Li}$  relaxation is slow, the effect is most likely, as indicated above, due to bimolecular carbon–lithium bond exchange. Density matrix equations were derived to calculate the  $^{13}\text{C}_\alpha$  NMR line shape of  $2\text{b}$ , taking into account the dynamics of intermolecular carbon–lithium bond exchange.<sup>23,27</sup> Since  $2\text{b-}^6\text{Li}$  contains  $^{13}\text{C}_\alpha$  in natural abundance, the faster of the exchange processes is the mutual exchange of  $^6\text{Li}$ 's between a  $^{12}\text{C}_\alpha$  and a  $^{13}\text{C}_\alpha$ . As far as calculating the  $^{13}\text{C}_\alpha$  resonance is concerned, the exchange process is best simulated as (2) shown together with the product spin states,  $\phi$ , of the different species:



$$\phi \begin{cases} \alpha/l & m & \alpha m & l \\ \beta/l & m & \beta m & l \end{cases}$$

where  $\alpha$  and  $\beta$  are states of  $^{13}\text{C}$  and  $l$  and  $m$  are states of  $^6\text{Li}$ .

One takes all elements of the density matrix equation for the " $^{13}\text{C-}^6\text{Li}$  (5) diagonal in  $^6\text{Li}$  between  $^{13}\text{C}$  states connected by a  $\Delta m_z = +1$  transition. The required elements of the density

$$\langle \alpha/l | i[\rho_g^{\text{CLi}} \mathcal{A}] + \rho^{\text{CLi}}/T + E\rho^{\text{CLi}} | \beta/l \rangle = 0 \quad (5)$$

matrix  $\langle \alpha/l | \rho^{\text{CLi}} | \beta/l \rangle$  are for the transitions  $\alpha(+1) \rightarrow \beta(+1)$ ,  $\alpha(0) \rightarrow \beta(0)$ , and  $\alpha(-1) \rightarrow \beta(-1)$ , abbreviated **1**, **2**, and **3**, respectively, where the spin states of  $^6\text{Li}$  are given by their  $m_z$  values. The exchange term is given as (6) where  $ae$  means after

$$[E\rho^{\text{CLi}}]_{ij} = k_1[(\rho^{\text{CLi}}(ae) - \rho^{\text{CLi}})]_{ij} \quad (6)$$

exchange and  $k_1$  is the pseudo-first-order rate constant. For exchange step (2), an element of  $\rho^{\text{CLi}}$  before exchange may be written as (7), recalling that  $\text{Tr}\rho = 1$ , and  $m$  sums over all states

$$\rho_{\alpha l, \beta l}^{\text{CLi}} = \rho_{\alpha l, \beta l}^{\text{CLi}} \sum_m \rho_{m, m}^{\text{CLi}} \quad (7)$$

**Table 2.** First-Order Rate Constants for a Carbon–Lithium Bond Exchange,  $2\text{b-}^6\text{Li}$ , in  $\text{THF-}d_8$

$T$ (K)	$k_1(0.21 \text{ M})$ ( $\text{S}^{-1}$ )	$k_1(0.11 \text{ M})$ ( $\text{S}^{-1}$ )	$k_1(0.055 \text{ M})$ ( $\text{S}^{-1}$ )
300	26	14	6
305	28	16	8
310	37	20	14

of  $^6\text{Li}$ . The effect of exchange on an element of  $\rho^{\text{CLi}}$  is to permute  $l$  with  $m$  on the right hand side of (7); see (8). Since

$$\rho^{\text{CLi}}(ae)_{\alpha l \beta l} = \sum_m \rho_{\alpha m, \beta m}^{\text{CLi}} \rho_{l, l}^{\text{CLi}} \quad (8)$$

the diagonal elements of  $\rho^{\text{CLi}}$  are one-third each, the element of  $E\rho^{\text{CLi}}$  is given by (9). The resulting density matrix equations in

$$[E\rho^{\text{CLi}}]_{\alpha l \beta l} = k_1((1/3) \sum_{m(m \neq l)} \rho_{\alpha m, \beta m}^{\text{CLi}} - (2/3) \rho_{\alpha l, \beta l}^{\text{CLi}}) \quad (9)$$

matrix form are shown in (10) where  $\Delta\nu$  is  $\nu - \nu_{\text{ref}}$ ,  $1/T$  is the line width unperturbed by exchange,  $C$  is a constant, and the  $\rho^{\text{CLi}}$  elements have been abbreviated as  $\rho_i$  ( $i = 1, 2, 3$ ).

$$\begin{bmatrix} i2\pi(\Delta\nu - J) & 1/3k_1 & 1/3k_1 \\ -T^{-1} - 2/3k_1 & & \\ 1/3k_1 & i2\pi\Delta\nu & 1/3k_1 \\ & -T^{-1} - 2/3k_1 & \\ 1/3k_1 & 1/3k_1 & i2\pi(\Delta\nu + J) \\ & & -T^{-1} - 2/3k_1 \end{bmatrix} \times \begin{bmatrix} \rho_1 \\ \rho_2 \\ \rho_3 \end{bmatrix} = iC \begin{bmatrix} 1 \\ 1 \\ 1 \end{bmatrix} \quad (10)$$

The equations are solved for the  $\rho$  elements which are summed (11) to give the absorption. Comparison of calculated with experimental line shapes, Figure 8, provides the rate constants resulting in  $\Delta H^\ddagger$  and  $\Delta S^\ddagger$  of 10.8 kcal/mol and  $-20$  eu, respectively. Line shapes were also recorded for three

$$\text{Abs}(\Delta\nu) = -\text{Im}(\rho_1 + \rho_2 + \rho_3) \quad (11)$$

concentrations of  $2\text{b}$ , 0.21, 0.11, and 0.05 M. Despite the small coupling, 3.8 Hz, undergoing averaging, it is clear from the data, Table 2, that  $k_1$  is linear with the concentration of  $2\text{b}$ , consistent with the proposed bimolecular exchange process.

Inspection of Table 1 shows that the different dynamic processes uncovered for  $2\text{b}$  take place at markedly different rates,  $k_1$  (apparent) ( $\text{s}^{-1}$ ) at 250 K being  $1.09 \times 10^4$ , 80, and 0.044 for, respectively, ion–ion reorientation, phenyl–benzyl rotation, and bimolecular carbon–lithium bond exchange, showing these processes are not correlated. Slower processes are most likely accompanied by aspects of mechanisms of the faster processes. For example, while reorientation transfers coordinated Li between two sides of the benzyl plane, it does not disrupt the  $\pi$  structure associated with the ring–benzyl bond. In contrast, bimolecular carbon–lithium bond exchange may well be accompanied by the faster rotation around the ring– $\text{C}_\alpha$  bond. The transition states for the three dynamic processes must involve changes in the  $\text{C}_\alpha$ –Li ionic character compared to the ground state; it should increase during reorientation and decrease with rotation around the ring– $\text{C}_\alpha$  bond. A more detailed understanding of these mechanisms must follow further studies.

## Conclusion

The observation and magnitude of spin coupling between  $^{13}\text{C}_\alpha$  and  $^6\text{Li}$ , or of its manifestation in several benzylic lithium

(27) Fraenkel, G. In *Techniques in Chemistry, Investigation in Rates and Mechanisms of Reactions*, 4th ed.; Bernasconi, D. F., Ed.; Wiley-Interscience: New York, 1986; Part 2, pp 357–604.

compounds, under conditions where bimolecular carbon–lithium bond exchange is slow, are taken as evidence that the C<sub>α</sub>–Li bond is detectably covalent though to a lesser degree than in monomeric RLi species wherein <sup>1</sup>J(<sup>13</sup>C–<sup>6</sup>Li) is 16 Hz, as evidenced also by the aromatic <sup>13</sup>C ring shifts.<sup>28</sup> This places benzylic lithium compounds as the missing link in carbon–lithium covalency. Carbon–lithium bond exchange is slow for internally solvated benzylolithiums as well as for benzylolithium-<sup>13</sup>C<sub>α</sub> (selectively enriched), dilute and at low temperature.

NMR line shape analysis reveals the dynamics of bimolecular carbon–lithium bond exchange, first-order rotation around the phenyl–C<sub>α</sub> bonds, and transfer of coordinated Li between two sides of the benzyl plane, the three processes listed in order of increasing rates.

## Experimental Section

**Materials.** Deuterated solvents and (α-<sup>13</sup>C)toluene came from Cambridge Isotopes; lithium (96% <sup>6</sup>Li) was from Oak Ridge National Laboratory. Dr. Jose Cabral prepared the bis(2-methoxyethyl)methylamine. Chloro(chloromethyl)dimethylsilane was purchased from Petrarch Systems; bis(2-methoxyethyl)amine was from Fluka. All other materials were purchased from Aldrich Chemical Co. Toluene was distilled from CaH<sub>2</sub>, TMEDA was distilled from KOH, and the main fraction was distilled immediately before use from CaH<sub>2</sub>. Ethers and alkanes used in organometallic reactions were distilled from sodium benzophenone ketyl under an atmosphere of argon.

**Preparation and Handling of Organolithium Compounds.** The glassware used in the preparation or reaction of organolithium reagents was baked in an oven overnight; the glassware was assembled while it was still warm. The glassware was then flame dried under vacuum and flushed at least three times with purified argon with the use of a Firestone valve. Syringes were dried overnight in an oven and assembled while still warm. The needles were then placed in a flask filled with argon until the syringe was cool. Organolithium compounds were handled either in Schlenk flasks or in a drybox.

**Titration of Organolithium Compounds.** Organolithium reagents were titrated for both total base content and alkoxide content. The total amount of base was determined by adding a 1 mL sample of organolithium solution to a solution of menthol in THF. The base was then titrated with a 0.1 M solution of benzoic acid in toluene with methylene blue as an indicator. The amount of alkoxide was then determined by first quenching the organolithium sample with allyl bromide and then carrying out a similar titration. The concentration of carbon-bound base is the difference between these titrations.

**Preparation of NMR Samples.** NMR sample tubes were connected to a 14/20 joint with a short section of hard glass with an outside diameter of 5 mm. The tubes were dried in an oven overnight. An adapter was then attached to the tube, and it was evacuated to approximately 5 μm and flamed dried. The tube and sample were then transferred into the drybox. The sample was introduced into the tube either as a solid or in solution. The tube was then attached to the high-vacuum line, residual solvent was slowly distilled out, and then the tube was evacuated to below 5 μm. Deuterated solvent, previously dried with sodium and benzophenone, was then vacuum transferred into the NMR tube. The resulting solution was degassed by using two freeze–pump–thaw cycles. The sample was frozen with liquid nitrogen, the headspace was evacuated, and the tube was sealed off using a small hot pinpoint flame.

**NMR Parameters.** NMR spectroscopy was performed on a Bruker MSL-300. Relevant parameters are as follows:

	<sup>13</sup> C		<sup>6</sup> Li
	aromatic and benzyl	ligand and silyl	
frequency, MHz	75	75	44
transform, K	64	64	8
spectral width, Hz	3760	15151	4000
resolution, Hz/point	0.115	0.462	0.977
pulse width, μs	5.0	5.0	6.0
acquisition time, s	4.36	1.08	1.02
transients	1600–9600	1600–6400	200

The <sup>6</sup>Li{<sup>1</sup>H} NOE experiments were performed by irradiating the indicated protons with a 2.0 mW pulse for 3.0 s. The enhancements of the <sup>6</sup>Li spectra were measured as a percentage compared to a reference spectrum taken when the irradiation was done at a frequency at which there was no proton resonance.

**Synthesis of *n*-Butyl(<sup>6</sup>Li)lithium.** Enriched lithium (96% <sup>6</sup>Li) (1.51 g, 251 mmol) was cut into pea-sized pieces in the drybox (argon atmosphere) and placed in a 250 mL Erlenmeyer flask equipped with a rubber septum. The flask was removed from the drybox and placed under argon from an inlet. Pentane (60 mL) and *n*-butyl bromide (6.4 mL, 60 mmol) were introduced using a syringe. The mixture was placed in an ultrasound apparatus until all of the reaction was complete (ca. 4 h). The reaction was monitored by removing a small sample and quenching with water; the organic layer was then checked for butyl bromide by gas chromatography. The purple precipitate which had developed in the reaction mixture was allowed to settle overnight. The pentane layer was removed with a syringe and split into two centrifuge tubes equipped with rubber septa, and the last remnants of precipitate were removed by centrifuging for 30 min. The pentane layer was removed with a syringe and transferred under argon into a flame-dried 100 mL Schlenk flask equipped with a glass stopcock. The precipitate was washed with additional pentane (10 mL). The solution was titrated as explained in the previous section. The sample was 0.832 M in total base and 0.004 M in alkoxide, the overall yield of 0.828 M carbon-bound base being 96% based on butyl bromide.

**α-(Trimethylsilyl)toluene, 9.** A 500 mL three-neck round bottom flask was equipped with a condenser, a glass stopcock, and an argon inlet. After flame drying under argon, the flask was charged with a solution of TMEDA (10.2 mL, 67.6 mmol) in toluene (200 mL, 1.88 mol); a 2.5 M solution of *n*-butyllithium in hexane (27.0 mL, 67.5 mmol) was then added. The solution was heated at 90 °C for 1 h. After the resulting red solution was cooled to room temperature, freshly distilled chlorotrimethylsilane (9.6 mL, 75.6 mmol) was added, and the solution was left to stir overnight. Excess toluene was removed by distillation through a 30 cm Vigreux column. The remaining solution was then placed in a smaller pot, and the product was fractionally distilled at normal pressure to yield a clear liquid (9.98 g, 62%): bp 175–180 °C (lit.<sup>29</sup> bp 93 °C (35 Torr)); <sup>1</sup>H NMR (CDCl<sub>3</sub>, 200 MHz) δ 7.31–7.03 (structured m, 5 H), 2.13 (s, 1 H), 0.68 (s, 9 H); <sup>13</sup>C NMR (CDCl<sub>3</sub>, 50.3 MHz) δ 141, 128.4, 128.2, 124, 27, –1.8.

**[α-(Trimethylsilyl)benzyl]lithium·TMEDA Complex, 6.** A 20 mL Schlenk flask equipped with a Firestone valve and a glass stopcock was charged via a syringe with a solution of α-(trimethylsilyl)toluene (0.50 mL, 2.7 mmol) and TMEDA (0.38 mL, 2.5 mmol) in diethyl ether (5.0 mL). After cooling to –70 °C, a 2.5 M solution of *n*-butyllithium (1.0 mL, 2.5 mmol) was added by syringe. The solution was stirred at –70 °C for 1 h and at room temperature overnight. The ether was removed via house vacuum and then replaced with pentane. At this time a solid precipitate formed. The solvent was removed with a syringe, and the precipitate was washed with two portions (5 mL) of pentane. The last traces of solvent were removed by pumping under vacuum (1.5 Torr), and the solid was transferred to the drybox. An NMR sample, 80 mg in 3.8 mL of (<sup>2</sup>H<sub>10</sub>) diethyl ether (0.073 M), was prepared as outlined above: <sup>1</sup>H NMR (Et<sub>2</sub>O-*d*<sub>10</sub>, 303 K, 300 MHz) δ 6.59 (t, *J* = 7.1 Hz, 2 H), 6.34 (d, *J* = 7.5 Hz, 2 H), 5.81 (t, *J* = 7.1 Hz, 1 H), 2.34 (s, 4 H), 2.13 (s, 12 H), –0.03 (s, 9 H); <sup>13</sup>C NMR (Et<sub>2</sub>O-*d*<sub>10</sub>, 300 K, 75.5 MHz) δ 157.2, 130.1, 119.2, 109.7, 57.6, 45.6, 41.5, 2.5.

**[α-(Trimethylsilyl)benzyl]lithium·Bis(2-methoxyethyl)methylamine Complex.** A 20 mL Schlenk flask equipped with a Firestone valve and a glass stopcock was charged via syringe with a solution of α-(trimethylsilyl)toluene (0.92 mL, 5.0 mmol) and bis(2-methoxyethyl)methylamine (0.74 g, 5.0 mmol) in diethyl ether (5.0 mL). A 2.5 M solution of *n*-butyllithium (2.0 mL, 5.0 mmol) was added by syringe.

(28) Preliminary results of calculations of C–Li bond order and “s” character for benzylolithium compared to vinylolithium for which <sup>1</sup>J(<sup>13</sup>C–<sup>6</sup>Li) is 16 Hz in monomers are consistent with a <sup>13</sup>C<sub>α</sub>–<sup>6</sup>Li coupling of ca. 3 Hz in benzylolithium and by this treatment imply that the reduction in the coupling constant is due to decreases in both bond order (16%) and “s” character (78%). Professor P. v. R. Schleyer and Dr. N. J. R. Van Eikema Hommes, University of Erlangen. Private communication.

(29) Gilman, H.; Marshall, F. J. *J. Am. Chem. Soc.* **1949**, *71*, 2066.

The solution was stirred at room temperature overnight. Then, the ether was removed via house vacuum and then replaced with pentane. At this time a solid precipitate formed. The solvent was removed with a syringe. The precipitate was washed with two portions (5 mL) of pentane. The last traces of solvent were removed by pumping under vacuum (1.5 Torr), and the solid was transferred to the drybox. An NMR sample, 34 mg in 1.0 mL of (<sup>2</sup>H<sub>10</sub>)diethyl ether (0.20 M), was prepared as outlined above: <sup>1</sup>H NMR (Et<sub>2</sub>O-*d*<sub>10</sub>, 303 K, 300 MHz) δ 6.46 (t, *J* = 7.1 Hz, 2 H), 6.31 (d, *J* = 7.4 Hz), 5.69 (td, *J* = 5.8 Hz, 1.0 Hz, 1 H), 3.48 (t, *J* = 5.4 Hz), 3.24 (s, 6 H), 2.53 (t, *J* = 5.4 Hz), 2.22 (s, 3 H), 1.40 (s, 1 H), -0.04 (s, 9 H); <sup>13</sup>C NMR (Et<sub>2</sub>O-*d*<sub>10</sub>, 303 K, 75.5 MHz) δ 150.0, 128.7, 128.1, 120.7, 108.0, 71.9, 58.9, 57.7, 43.6, 40.5, -0.5.

**α-[(Chloromethyl)dimethylsilyl]toluene, 4a.** A 500 mL three-neck flask equipped with a condenser, an addition funnel, an argon inlet, and a magnetic stirbar was charged with commercial magnesium shavings (2.44 g, 100 mmol) which were then covered with Et<sub>2</sub>O (100 mL). Benzyl chloride (8.8 mL, 76 mmol) in Et<sub>2</sub>O (100 mL) was added through the addition funnel at such a rate as to maintain a steady reflux (*ca.* 30 min). The mixture was heated to reflux for an additional 2 h and then cooled to room temperature. Chloro(chloromethyl)dimethylsilane (10.0 mL, 76 mmol) in Et<sub>2</sub>O (20 mL) was added through the addition funnel over 30 min, and then the mixture heated to reflux overnight. After cooling to room temperature, the reaction was carefully quenched with 2 N aqueous HCl (200 mL). After separation of layers, the aqueous phase was extracted with Et<sub>2</sub>O (100 mL). The combined organic phases were washed with H<sub>2</sub>O (100 mL), saturated aqueous NaHCO<sub>3</sub> (100 mL), and brine (100 mL). The ethereal layer was dried by passing through Drierite and then concentrated *in vacuo*. The remaining liquid was vacuum distilled through a Vigreux column. The first fraction yield α-(trimethylsilyl)toluene as a clear liquid (1.26 g, 44% yield): bp 37–40 °C (0.8 Torr). The second fraction yielded α-[(chloromethyl)dimethylsilyl]toluene as a clear liquid (7.35 g, 48% yield): bp 57–60 °C (0.8 Torr) [lit.<sup>30</sup> bp 89–90 °C (4 Torr)]; <sup>1</sup>H NMR (CDCl<sub>3</sub>, 200 MHz) δ 7.29–7.26 (m, 2 H) 7.24–7.14 (m, 3 H), 2.75 (s, 2 H), 2.24 (s, 2 H), 0.11 (s, 6 H); <sup>13</sup>C NMR (CDCl<sub>3</sub>, 50.0 MHz) δ 138.9, 128.4, 128.1, 124.4, 29.5, 23.5, -4.9; mass spectrum, exact mass for C<sub>10</sub>H<sub>15</sub>ClSi, *m/e* calculated 198.0633, observed 198.0643. Note: the α-(trimethylsilyl)toluene resulted from the α-[(chloromethyl)dimethylsilyl]toluene reacting with the excess magnesium; it would be advisable to either use only a stoichiometric amount of magnesium or remove the initial Grignard reagent from the excess magnesium.

**α-[[Bis(2-methoxyethyl)amino]methyl]dimethylsilyl]toluene, 5a.** A solution of α-[(chloromethyl)dimethylsilyl]toluene (7.35 g, 36.8 mmol) in bis(2-methoxyethyl)amine (17 mL, 116 mmol) was heated in a 100 mL one-neck flask, equipped with a condenser and an argon inlet, to 120 °C overnight. The resulting hydrochloride salts of the amines were quenched with 2 N aqueous KOH (40 mL). The free amines were then extracted with CHCl<sub>3</sub> (3 × 50 mL), and the combined organic layers dried by passing through Drierite and then concentrated *in vacuo*. The remaining liquid was vacuum distilled through a Vigreux column. The first fraction yielded recovered bis(2-methoxyethyl)amine as a clear liquid (2.75 g, 20 mmol): bp 25–27 °C (0.45 Torr). The second fraction was α-[[bis(2-methoxyethyl)amino]methyl]dimethylsilyl]toluene, a clear liquid (8.63 g, 80%): bp 114–116 °C (0.45 Torr); <sup>1</sup>H NMR (CDCl<sub>3</sub>, 200 MHz) δ 7.26–7.00 (m, 5 H), 3.44 (t, *J* = 6.2 Hz, 4 H), 3.33 (s, 6 H), 2.65 (t, *J* = 6.2 Hz, 4 H), 2.14, 2.09 (overlapping s's, 4 H), 0.01 (s, 6 H); <sup>13</sup>C NMR (CDCl<sub>3</sub>, 50.0 MHz) δ 139.8, 128.0, 127.9, 123.7, 70.9, 58.5, 57.1, 45.4, 24.9, -3.3; mass spectrum, exact mass for C<sub>16</sub>H<sub>29</sub>NO<sub>2</sub>Si, *m/e* calculated 295.1969, observed 295.1970.

**[α-[[Bis(2-methoxyethyl)amino]methyl]dimethylsilyl]benzyl]-(<sup>6</sup>Li)lithium, 2a.** A 40 mL Schlenk flask equipped with a Firestone valve and a glass stopcock was charged by a syringe with a solution of α-[[bis(2-methoxyethyl)amino]methyl]dimethylsilyl]toluene (0.88 g, 2.96 mmol) in diethyl ether (10.0 mL). A 2.8 M solution of *n*-butyl(<sup>6</sup>Li)lithium in pentane (1.0 mL, 2.8 mmol) was slowly added by syringe; the reaction is slightly exothermic at room temperature. Even though a precipitate formed almost immediately, the reaction was stirred for an additional 15 min. The precipitate was allowed to settle, and then the ether was syringed out. The precipitate was washed with two

more 10 mL portions of ether. After the last traces of solvent were removed *in vacuo*, the solid was transferred to the drybox. An NMR sample of 90 mg in 4.0 mL of THF-*d*<sub>8</sub> was prepared as noted previously (0.075 M): <sup>1</sup>H NMR (THF-*d*<sub>8</sub>, 293 K, 300 MHz) δ 6.48 (structured m, 2 H), 6.31 (structured m, 2 H), 5.69 (structured m, 1 H), 3.46 (t, *J* = 5.4 Hz, 4 H), 3.10 (s, 6 H), 2.62 (t, *J* = 5.4 Hz, 4 H), 2.06 (s, 2 H), 1.50 (s, 1 H), -0.07 (s, 6 H); <sup>13</sup>C NMR (THF-*d*<sub>8</sub>, 230 K, 75.5 Hz) δ 158.6, 128.5, 128.3, 121.8, 117.5, 107.1, 69.6, 58.7, 56.5, 46.8, 36.7, -0.5.

***p*-tert-Butyl-α-[(chloromethyl)dimethylsilyl]toluene, 4b.** A 250 mL three-neck flask equipped with a condenser, an addition funnel, an argon inlet, and a magnetic stirbar was charged with commercial magnesium shavings (1.32 g, 54.3 mmol) which were then covered with Et<sub>2</sub>O (40 mL). A solution of α-bromo-*p*-tert-butyltoluene (10.0 mL, 54.4 mmol) in Et<sub>2</sub>O (40 mL) was added from the addition funnel at such a rate as to maintain a steady reflux (*ca.* 60 min). The mixture was heated to reflux for 1 h and then cooled to room temperature. The ethereal layer was then added via a cannula to a solution of chloro-(chloromethyl)dimethylsilane (8.0 mL, 61 mmol) in Et<sub>2</sub>O (40 mL). After the reaction was allowed to stir overnight, the resulting salt was removed by filtration. The ether was removed *in vacuo* to give a white semisolid. Recrystallization from ether gave a white solid (3.36 g, 42%): mp 148–151 °C; <sup>1</sup>H NMR (CDCl<sub>3</sub>, 200 MHz) δ 7.35 (d, *J* = 8.4 Hz, 2 H), 7.22 (d, *J* = 8.4 Hz, 2 H), 2.91 (s, 2 H), 1.34 (s, 9 H). The <sup>1</sup>H NMR spectrum is consistent with the Wurtz coupled product. The mother liquor from the recrystallization was concentrated *in vacuo*, and the remaining liquid was vacuum distilled to give *p*-tert-butyl-α-[(chloromethyl)dimethylsilyl]toluene (4.75 g, 34%): bp 92–95 °C (0.75 Torr); <sup>1</sup>H NMR (CDCl<sub>3</sub>, 250 MHz) δ 7.32 (d, *J* = 8.4 Hz, 2 H), 7.03 (d, *J* = 8.4 Hz, 2 H), 2.81 (s, 2 H), 2.26 (s, 2 H), 1.38 (s, 9 H), 0.18 (s, 6 H); <sup>13</sup>C NMR (CDCl<sub>3</sub>, 62.9 MHz) δ 147.1, 135.6, 127.8, 125.6, 34.2, 31.5, 29.6, 22.9, -4.8; mass spectrum for C<sub>14</sub>H<sub>23</sub>ClSi, *m/e* calculated for 254.1259, observed 254.1260.

***p*-tert-Butyl-α-[[bis(2-methoxyethyl)amino]methyl]dimethylsilyl]toluene, 5b.** A solution of *p*-tert-butyl-α-[(chloromethyl)dimethylsilyl]toluene (4.57 g, 17.8 mmol) in bis(2-methoxyethyl)amine (6.6 mL, 45 mmol) in a 100 mL one-flask, equipped with a condenser and an argon inlet, was heated to 100 °C overnight. The resulting hydrochloric salt of the amines was quenched with 2 N aqueous KOH (20 mL). After the free amines were extracted with chloroform (3 × 25 mL), the combined organic layers were dried by passing through Drierite and then concentrated *in vacuo*. The remaining liquid was vacuum distilled through a Vigreux column. The first fraction yielded some recovered bis(2-methoxyethyl)amine as a clear liquid (1.31 g, 10 mmol): bp 29–31 °C (1.0 Torr). The second fraction was *p*-tert-butyl-α-[[bis(2-methoxyethyl)amino]methyl]dimethylsilyl]toluene as a clear liquid (4.55 g, 73%): bp 146–149 °C (1.0 Torr); <sup>1</sup>H NMR (CDCl<sub>3</sub>, 250 MHz) δ 7.24 (d, *J* = 8.3 Hz, 2 H), 6.97 (d, *J* = 8.3 Hz, 2 H), 3.45 (t, *J* = 6.2 Hz, 4 H), 3.34 (s, 6 H), 2.67 (t, 6.2 Hz, 4 H), 2.11 (s, 4 H), 1.32 (s, 9 H), 0.06 (s, 6 H); <sup>13</sup>C NMR (CDCl<sub>3</sub>, 62.9 MHz) δ 146.6, 136.7, 127.9, 124.9, 71.1, 58.7, 57.3, 45.7, 34.1, 31.4, 24.4, -3.0; mass spectrum for C<sub>20</sub>H<sub>37</sub>NO<sub>2</sub>Si, *m/e* calculated 351.2595, observed 351.2603.

**[*p*-tert-Butyl-α-[[bis(2-methoxyethyl)amino]methyl]dimethylsilyl]benzyl]-(<sup>6</sup>Li)lithium, 2b.** A 20 mL Schlenk flask equipped with a Firestone valve and a glass stopcock was charged via a syringe under argon with a solution of *p*-tert-butyl-α-[[bis(2-methoxyethyl)amino]methyl]dimethylsilyl]toluene (1.09 g, 3.08 mmol) in diethyl ether (5.0 mL). A 0.89 M solution of *n*-butyl(<sup>6</sup>Li)lithium (3.5 mL, 3.1 mmol) was slowly added by syringe; the reaction is slightly exothermic at room temperature. Even though a precipitate formed almost immediately, the reaction was stirred for an additional 15 min. The precipitate was allowed to settle, and then the ether was removed by a syringe. The precipitate was washed with two more 5 mL portions of ether. The last traces of solvent were removed *in vacuo*, and the solid was transferred to the drybox. An NMR sample of 86 mg in 2.8 mL of THF-*d*<sub>8</sub> (0.086 M) was prepared as described previously: <sup>1</sup>H NMR (THF-*d*<sub>8</sub>, 315 K, 300 MHz) δ 6.59 (d, *J* = 8.4 Hz, 2 H), 6.29 (d, *J* = 8.4 Hz, 2 H), 3.44 (t, *J* = 5.4 Hz, 4 H), 3.07 (s, 6 H), 2.62 (t, *J* = 5.4 Hz, 4 H), 2.06 (s, 2 H), 1.43 (s, 1 H), 1.13 (s, 9 H), -0.03 (s, 6 H); <sup>13</sup>C NMR (THF-*d*<sub>8</sub>, 180 K, 75.5 MHz) δ 156.0, 128.6, 125.0, 124.8, 121.1, 116.1, 69.2, 59.0, 57.5, 55.3, 46.9, 34.2, 33.8, 32.3, 1.1, -2.1.



**[3-[Bis(2-methoxyethyl)amino]propyl]benzene, 11.** A solution of 1-chloro-3-phenylpropane (7.03 g, 45.5 mmol) in bis(2-methoxyethyl)amine (20 mL, 137 mmol) in a 100 mL one-neck flask, equipped with a condenser and an argon inlet, was heated to 125 °C overnight. The resulting hydrochloride salts of the amines were quenched with 2 N aqueous KOH (45 mL). The free amines were then extracted with ethyl acetate (3 × 50 mL), and the combined organic layers were dried by passing through Drierite and concentrated *in vacuo*. The remaining liquid was vacuum distilled through a Vigreux column. The first fraction consisted of recovered bis(2-methoxyethyl)amine, a clear liquid (4.64 g, 34.8 mmol): bp 25–27 °C (0.7 Torr). The second fraction was [3-[bis(2-methoxyethyl)amino]propyl]benzene as a clear liquid (9.83 g, 86%): bp 115–117 °C (0.7 Torr); <sup>1</sup>H NMR (CDCl<sub>3</sub>, 200 MHz) δ 7.31–7.12 (m, 5 H), 3.43 (t, *J* = 6.1 Hz, 4 H), 3.32 (s, 6 H), 2.70 (t, *J* = 6.1 Hz, 4 H), 2.64–2.53 (m, 4 H), 1.86–1.71 (m, 2 H); <sup>13</sup>C NMR (CDCl<sub>3</sub>, 50.0 MHz) δ 142.2, 128.2, 128.1, 125.5, 71.1, 58.6, 54.6, 53.8, 22.4, 28.6; mass spectrum for C<sub>15</sub>H<sub>25</sub>NO<sub>2</sub>, *m/e* calculated 251.1887, observed 251.1886.

**[[3-[Bis(2-methoxyethyl)amino]propyl]benzyl]<sup>6</sup>Li)lithium, 7.** A 20 mL Schlenk flask equipped with a Firestone valve and a glass stopcock was charged via a syringe with a solution of [3-[bis(2-methoxyethyl)amino]propyl]benzene (1.24 g, 4.93 mmol) in diethyl ether (10 mL). A 0.98 M solution of *n*-butyl(<sup>6</sup>Li)lithium (5.0 mL, 4.9 mmol) was then slowly added by syringe; the reaction is slightly exothermic at room temperature. Even though a precipitate formed almost immediately, the reaction was stirred for an additional 15 min. After the precipitate was allowed to settle, the ether was removed using a syringe. The precipitate was washed with two more 10 mL portions of ether. The last traces of solvent were removed *in vacuo*, and the solid was transferred to the drybox. An NMR sample of 86 mg in 3.8 mL of THF-*d*<sub>8</sub> (0.088 M) was prepared as described previously: <sup>1</sup>H NMR (THF-*d*<sub>8</sub>, 294 K, 300 MHz) δ 6.24 (br s [due to slow rotation around the *ipso*-benzyl bond], 2 H), 5.79 (br s [due to slow rotation around the *ipso*-benzyl bond], 2 H), 5.17 (structured m, 1 H), 3.41 (t, *J* = 5.3 Hz, 4 H), 3.18 (s, 6 H), 2.59 (t, *J* = 5.3 Hz, 4 H), 2.58–2.44 (m, 2 H), 2.09–2.07 (m, 2 H), 1.70 (s, 1 H); <sup>13</sup>C NMR (THF-*d*<sub>8</sub>, 210 K, 75.5 MHz) δ 155.6, 129.3, 127.6, 117.0, 108.0, 100.9, 69.5, 67.4, 58.6, 54.8, 53.3, 29.8.

**Benzyl(<sup>6</sup>Li)lithium·TMEDA Complex, 8.** A 20 mL Schlenk flask equipped with a Firestone valve and a glass stopcock was charged via

a syringe with a solution of toluene (0.98 mL, 9.2 mL) in TMEDA (1.4 mL, 9.3 mmol). A 0.77 M solution of *n*-butyl(<sup>6</sup>Li)lithium (12.0 mL, 9.2 mmol) was added, and the reaction mixture was stirred for 2 days. The resulting precipitate was allowed to settle, and the solvent was removed with a syringe. The precipitate was washed with two 10 mL portions of pentane. The solvent was removed *in vacuo*, and the solid was then brought into the drybox. An NMR sample of 34 mg in 0.8 mL of THF-*d*<sub>8</sub> (0.20 M) was prepared as described previously; <sup>1</sup>H NMR (THF-*d*<sub>8</sub>, 260 K, 300 MHz) δ 6.27 (td, *J* = 6.9, 1.5 Hz, 2 H), 6.05 (dd, *J* = 8.2, 1.1 Hz, 2 H), 5.35 (td, *J* = 6.9, 1.5 Hz, 1 H), 2.29 (s, 4 H), 2.15 (s, 12 H), 1.55 (s, 2 H); <sup>13</sup>C NMR (THF-*d*<sub>8</sub>, 260 K, 75.5 MHz) δ 161.1, 128.3, 116.6, 104.3, 58.6, 46.4, 37.1.

**( $\alpha$ -<sup>13</sup>C)Benzyl(<sup>6</sup>Li)lithium·TMEDA Complex, 8-<sup>13</sup>C $\alpha$ .** A 20 mL Schlenk flask equipped with a Firestone valve and a glass stopcock was placed in a drybox and then charged with a solution of ( $\alpha$ -<sup>13</sup>C)-toluene (0.50 mL, 4.9 mmol) in TMEDA (0.80 mL, 5.3 mmol). A 0.83 M solution of *n*-butyl(<sup>6</sup>Li)lithium in pentane (6.0 mL, 5.0 mmol) was then added using a syringe, and the reaction mixture was stirred for 2 days. The resulting precipitate was allowed to settle, and then the solvent was removed via a syringe. The precipitate was washed with two 10 mL portions of pentane. The excess solvent was removed *in vacuo*. An NMR sample of 3 mg in 3.2 mL of Et<sub>2</sub>O-*d*<sub>10</sub> (0.005 M) was prepared as explained previously: <sup>1</sup>H NMR (THF-*d*<sub>8</sub>, 303 K, 300 MHz) δ 6.27 (td, *J* = 6.9, 1.5 Hz, 2 H), 6.05 (ddd, *J* = 8.2, 3.0, 1.1 Hz, 2 H), 5.38 (td, *J* = 6.9, 1.5 Hz, 1 H), 2.29 (s, 4 H), 2.15 (s, 12 H), 1.55 (d, *J* = 132.7 Hz, 2 H); <sup>13</sup>C NMR (THF-*d*<sub>8</sub>, 303 K, 75.5 MHz) δ 161.1 (d, *J* = 140.2 Hz), 128.3 (s), 116.6 (d, *J* = 5.4 Hz), 104.8 (s), 58.7 (s), 46.2 (s), 36.6 (s).

**Acknowledgment.** This research was generously supported by the National Science Foundation, Grant Number CHE-9317298, as was also, in part, the purchase of the NMR equipment used in this work. We thank the Office of Research, The Ohio State University, for financial assistance. We are happy to acknowledge the expert technical help and advice of Dr. Charles Cottrell, Central Campus Instrumentation Center, The Ohio State University.

JA951866L